

1 **Comparative analysis of novel *Pseudobdellovibrionaceae* genera and species yields insights**
2 **into the genomics and evolution of bacterial predation mode**

3 Rebecca L. Maher^{a,b*}, Janna Wülbern^{c*}, Johannes Zimmermann^{c,d}, Emily Yeh^b, Liesl Benda^b,
4 Urska Repnik^e, Janina Fuß^f, Sven Künzel^g, Hinrich Schulenburg^{c,h}, Brendan J.M. Bohannan^b,
5 Karen L. Adair^{b*}, Julia Johnke^{c*}

6
7 **Affiliations**

8 ^aFriday Harbor Laboratories, University of Washington, Friday Harbor, Washington, USA

9 ^bInstitute of Ecology and Evolution, Department of Biology, University of Oregon, Eugene,
10 Oregon, USA

11 ^cEvolutionary Ecology and Genetics, Zoological Institute, Kiel University, Kiel, Germany

12 ^dCluster of Excellence Balance of the Microverse, Friedrich Schiller University, Jena, Germany

13 ^eCentral Microscopy, Department of Biology, Kiel University, Kiel, Germany

14 ^fInstitute of Clinical Molecular Biology (IKMB), Kiel University, Kiel, Germany

15 ^gMax Planck Institute for Evolutionary Biology, Plön, Germany

16 ^hAntibiotic Resistance Group, Max Planck Institute for Evolutionary Biology, Plön, Germany

17 * Shared first or senior authors

18 Correspondence: Julia Johnke, jjohnke@zoologie.uni-kiel.de

19

20

21

22

23

24

25

26 **Abstract**

27 Bacteria of the family *Pseudobdellovibrionaceae* belong to a group of bacteria that kill and feed
28 on other bacteria. The diversity of predation strategies, habitats, and genome characteristics of
29 these bacteria are largely unexplored, despite their ecological and evolutionary importance in
30 microbial communities. Therefore, we characterized new *Pseudobdellovibrionaceae* strains
31 isolated from the direct environments of three animal hosts: the zebrafish (*Danio rerio*), the
32 threespine stickleback fish (*Gasterosteus aculeatus*), and the nematode *Caenorhabditis elegans*.
33 We used transmission electron microscopy (TEM) and genomic analyses to characterize the
34 morphology and predation modes of our isolates. While most of our isolates exhibited
35 periplasmic (i.e. endoparasitic) predation, one isolate clearly exhibited epibiotic (i.e.
36 exoparasitic) predation and represents only the third confirmed epibiotic strain within its clade.
37 Of our isolates, six are members of five new species in the genus *Bdellovibrio* and two strains
38 likely represent new genera within the family *Pseudobdellovibrionaceae*. From metabarcoding
39 data, we found indications that *Pseudobdellovibrionaceae* are widespread among our three
40 animal hosts. Genomic analyses showed that epibiotic predators lack genes involved in host
41 independence (i.e. prey-independent feeding) and peptidoglycan modification. However, genes
42 unique to epibiotic predators may underlie this predation mode, particularly those involved in
43 cell wall remodeling and recycling. With robust phylogenomic analyses, we show that our novel
44 isolates cluster with previously described *Pseudobdellovibrionaceae* isolates according to
45 predation mode. Further, by placing *Pseudobdellovibrionaceae* predators within a wider
46 evolutionary history including other predatory and non-predatory bacteria, we postulate
47 periplasmic predation as the ancestral mode, with more derived epibiotic predators exhibiting
48 genome streamlining.

49

50 **Introduction**

51 For decades, researchers have documented the mechanisms by which top-down control
52 via predation drives structure and diversity in communities of plants and animals [1, 2]. More
53 recent evidence suggests that predation by bacteria may similarly structure microbial
54 communities, including those associated with animal hosts (e.g. in corals [3, 4]). Moreover, the
55 presence, abundance, and richness of bacterial predators are positively correlated with overall
56 microbiome diversity for numerous host-microbiome systems, most likely because predation on
57 highly abundant species allows rare taxa to thrive [5]. Understanding the potential contribution
58 of bacterial predators to host microbiome dynamics is important given the central role that
59 microbiomes can play in host health and well-being.

60 One of the best-studied bacterial predators, *Bdellovibrio bacteriovorus*, was discovered
61 over 60 years ago [6]. It is now considered a member of the “*Bdellovibrio* and like organisms”
62 (BALOs), a group of obligate predators of Gram-negative bacteria. Since then, detailed
63 information has been obtained on the distribution of BALOs across terrestrial and aquatic
64 habitats and their complex strategies of predation, growth, and reproduction [7, 8]. BALOs play
65 a role in microbial population control and nutrient cycling through substantial contributions to
66 bacterial death, despite their relatively low abundance [9]. However, most BALO research has
67 been restricted to a few type strains, and we are only beginning to uncover and comprehensively
68 describe the taxonomic and genetic diversity of BALOs [10]. For instance, our understanding of
69 bacterial predation modes largely reflects research done with two type strains from the
70 *Pseudobdellovibrionaceae* family (formerly *Bdellovibrionaceae* [11, 12]): the periplasmic
71 predator *B. bacteriovorus* HD100 and the epibiotic predator *Pseudobdellovibrio. exovorus* JSS.
72 Both predators employ a biphasic lifestyle including an attack phase in which the small, motile
73 predator cells actively search for prey cells. Once anchored to the prey cell, a periplasmic
74 predator enters the prey periplasm, forms a *bdelloplast*, and grows by consuming the prey's
75 cellular components. Then, the predator cell replicates, septates, and lyses the *bdelloplast*,

76 releasing offspring cells. In contrast, epibiotic predators attach to the prey cell and consume the
77 prey's cytoplasmic content without intrusion. The epibiotic predator *P. exovorus* then undergoes
78 binary or non-binary fission [13] and produces two to three attack phase daughter cells.

79 Next-generation sequencing technologies have uncovered genomic signatures of
80 predation among the BALOs [14], and genetic elements that differentiate the periplasmic and
81 epibiotic predation modes [15]. In an initial evaluation, epibiotic predators were deficient in
82 numerous functions due to their smaller genomes compared to the periplasmic predators.
83 However, the recent genomic characterization of an epibiotic predator placed within the genus
84 *Bdellovibrio* with a larger genome suggests that the genomic diversity in epibiotic predators is
85 under sampled [16].

86 In order to expand our understanding of BALO taxonomic and genetic diversity,
87 especially in animal hosts, we isolated nine novel *Pseudobdellovibrionaceae* strains from the
88 immediate environments of three important model animal species: the zebrafish (*Danio rerio*),
89 the threespine stickleback fish (*Gasterosteus aculeatus*), and the nematode *Caenorhabditis*
90 *elegans*. We characterized these strains using microscopy across the life cycle to infer predation
91 mode. We surveyed metabarcoding data from all three animal hosts to infer the prevalence of
92 these novel strains. Finally, we sequenced and assembled the genomes of these
93 *Pseudobdellovibrionaceae* strains *de novo* and compared them to existing genomes of predators
94 of the genera *Bdellovibrio* and *Pseudobdellovibrio*. These analyses expand substantially on
95 previous comparative genomic analyses of predatory bacteria [14, 15, 17, 18], led to the formal
96 description of new genera and species within the family *Pseudobdellovibrionaceae*, and provide
97 the most comprehensive phylogenetic history to date of predation mode, revealing conserved
98 genomic features differentiating these two predation lifestyles.

99

100 **Methods**

101 All materials and methods can be found in the supplemental material.

102

103 **Results**

104 **Newly obtained *Pseudobdellovibrionaceae* isolates varied in size and predation mode**

105 From the direct environments of three animal hosts, we isolated 9 novel BALO strains
106 (Table 1). Transmission electron microscopy (TEM) after negative staining was employed to
107 confirm predation strategies (Figure 1, Figure S1). The presence of a bdelloplast containing at
108 least one BALO cell was considered an indication of periplasmic predation. Bacteria of all
109 isolates had a curved-rod (vibrioid) shape and all periplasmic strains had thicker flagellar
110 filaments, which likely represent ensheathed flagella [19] and may help periplasmic predators to
111 retract their flagellum during prey invasion [20]. In contrast, the only epibiotic strain had a
112 notably thinner and longer flagellar filament, which suggests that this strain does not have a
113 sheathed flagellum. Moreover, flagellar waves differed between periplasmic predators and the
114 epibiotic *Bdellovampiro gaculeatus* SBM16 strain (see below for justification and a formal
115 description of all newly identified species). In detail, periplasmic predators showed the tapered
116 waves as described for *Bdellovibrio bacterivorus* [21, 22]. In contrast, the flagellum of
117 *Bdellovampiro gaculeatus* SBM16 consisted of homogenous waves with smaller amplitude.

118 The length of flagella and the size of predator cells varied between different strains
119 (Table 1) and across independent experiments of single strains (Table S1). Cells sampled after
120 the addition of fresh prey appeared larger and had a shorter flagellum than those from prey-
121 cleared standard overnight cultures. Variability in cell size within strains and even within the
122 same culture may be explained by an earlier observation that BALO flagella [23] and cells
123 continue to elongate after exiting the bdelloplast [24]. The negative correlation between
124 flagellum length and cell size is, however, puzzling. Notably, in the epibiotic strain, variation in

125 cell size was larger than in periplasmic strains, as illustrated by two differently sized attack phase
126 cells of SBM16 (Figure 1).

127 Between strains cell size and flagellum length showed no correlation (Table 1). For
128 example, the epibiotic *Bdellovampiro gaculeatus* strain SBM16 cells exhibited both a large cell
129 size ($0.77 \pm 0.24 \mu\text{m}^2$) and the longest flagellum ($7.13 \pm 1.57 \mu\text{m}$) among the analyzed strains
130 (Figure 1). In contrast, *Bdellovibrio tomkyle* strain MYbb1, despite having a small cell size (0.19
131 $\pm 0.02 \mu\text{m}^2$), had an average flagellum length ($3.02 \pm 0.22 \mu\text{m}$), while *Bdellovibrio bagaluti*
132 strain MYbb10 displayed a comparable flagellum length ($2.9 \pm 0.34 \mu\text{m}$) but a larger cell size
133 ($0.29 \pm 0.04 \mu\text{m}^2$) (Table 1, Figure S1). Notably, potential damage to the flagella during sample
134 preparation may have affected the measured flagellum lengths, possibly leading to
135 underestimation.

136 Cell shape was further assessed using the Feret diameter ratio, which indicates the degree
137 to which a particle is stretched or how similar its projected contour is to a circle, with higher
138 values suggesting elongated shape (Table 1). Notably, the highest values were recorded for
139 *Bdellovibrio krueschi* strain MYbb4, *Bdellovibrio kumpostii* strain MYbb5, *Bdellovibrio*
140 *bagaluti* strain MYbb10, and *Bdellovampiro gaculeatus* strain SBM16, indicating these cells
141 exhibited elongated or narrow morphologies compared to other BALO cells (Table 1).

142

143 **Comparative genomic analysis reveals novel *Pseudobdellovibrionaceae* genera and species**

144 To assign species and genus level taxonomic classifications to the novel strains, we used
145 average nucleotide identity (ANI) (>95% [25]) and average amino acid identity (AAI) (>65%
146 [26]). These comparative genomic analyses suggest novel genus and species relationships within
147 the *Pseudobdellovibrionaceae* family (Figure S2; Table S2). Building on previous work [12, 18],
148 AAI values support the existence of four genera within *Pseudobdellovibrionaceae* including
149 existing (*Bdellovibrio*, *Pseudobdellovibrio*) and novel genera (*Bdellovenatio*, *Bdellovampiro*).

150 Genus *Bdellovenatio* includes the novel strain *B. daniorerio* ZFWA1 which shares <62% AAI
151 with all other genomes. Genus *Bdellovampiro* includes novel and existing strains *B. gaculeatus*
152 SBM16 and *B. qaytius*, respectively, which share an AAI of 79.59%, and each have an AAI
153 <62% with *Pseudobdellovibrio exovor* JSS. *Bdellovibrio* species were confirmed for strains
154 MYbb10 and MYbb7 (now *B. bagaluti* strains MYbb10 and MYbb7), strains MYbb2 and *B.*
155 *bacteriovorus Tiberius* (now *B. tiberii* strains MYbb2 and Tiberius), and strains MYbb11 (now
156 *B. bacteriovorus* strain MYbb11), *B. bacteriovorus* 109J, and *B. bacteriovorus* HD100. Further,
157 the strains MYbb1 (now *B. tomkyle* strain MYbb1), MYbb4 (now *B. krueschi* strain MYbb4),
158 and MYbb5 (now *B. kumpostii* strain MYbb5) were identified as separate species. The results
159 also suggest that *B. bacteriovorus* strains SSB218315, kdesi, and W represent separate new
160 species. Notably, ANI values between 85%-95% are comparatively rare and represent a
161 discontinuity in the distribution of ANI values among closely related genomes [27]. A number of
162 genomes had ANI values within this range, including strains of *B. bacteriovorus*, *B. tiberii*, *B.*
163 *kumpostii*, and *B. sp* SSB218315, strains *B. sp* ZAP7 and *B. sp* KM01, and strains *B. sp* kdesi
164 and *B. tomkyle* MYbb1. While considered “species-like”, these sequence-discrete populations are
165 generally ecologically differentiated and still considered distinct species [27].

166

167 **Phylogenomic analysis identifies two distinct clades for periplasmic and epibiotic**

168 ***Pseudobdellovibrionaceae***

169 To uncover the ancestral predation mode in predatory bacteria, a tree with representative
170 outgroups including predatory and non-predatory bacteria, as well as one archaeon (Table S3),
171 was generated. The phylogenetic analysis led to the identification of two distinct clades, with one
172 clade containing all predatory bacteria with a periplasmic lifestyle (Figure 2a). *P. exovor* and
173 the non-predator *Oligoflexus tunisiensis* clustered within this clade as well. The other predatory
174 bacteria with a cooperative or epibiotic predation strategy (*Myxococcus xanthus*, *Micavibrio*

175 *aeruginosavorus*, and *Vampirovibrio chlorellavorus*) clustered within the second clade. It should
176 be noted that the genus *Micavibrio* is also part of the family *Pseudobdellovibrionaceae*. Our
177 phylogenomic analysis and others [12, 18] indicates that *Micavibrio* is not in close relation to the
178 known isolates of the genera *Bdellovibrio* and *Pseudobdellovibrio* nor to our newly isolated
179 strains and should be therefore re-classified. We are subsequently omitting *Micavibrio* from the
180 following focused analysis and whenever we discuss members of the family
181 *Pseudobdellovibrionaceae*.

182 We used core-genome sequence phylogenetic analysis to examine the evolutionary
183 relationships between 21 *Pseudobdellovibrionaceae* strains including our nine new isolates. The
184 maximum-likelihood phylogenetic tree was constructed based on the amino acid sequences of
185 1099 single-copy core genes (Figure 2b). *Pseudobdellovibrionaceae* strains fall into two distinct
186 clades that differentiate based on predation strategy. The novel epibiotic predator isolated from
187 the stickleback fish aquaculture water, here named *Bdellovampiro gaculeatus* strain SBM16,
188 clusters with known epibiotic predators *B. qaytius* and *P. exovorius*. The novel isolate from
189 zebrafish aquaculture water (*Bdellovenatio daniorerio* strain ZFWA1) was the most diverged
190 periplasmic *Pseudobdellovibrionaceae* strain.

191

192 **Epibiotic *Pseudobdellovibrionaceae* have distinct characteristics indicative of genome** 193 **reduction**

194 The predators included in Figure 2a were further explored by comparing genome
195 characteristics (Figure 3). Epibiotic *Pseudobdellovibrionaceae* genomes are smaller, have lower
196 GC content, and exhibit a higher coding density than most periplasmic
197 *Pseudobdellovibrionaceae* genomes (Figure 3a). Within the family, *P. exovorius* has the smallest
198 genome, while *B. qaytius* has the lowest GC content and highest coding density. Additionally,
199 all periplasmic predator genomes have less than 350 COGs categorized as M or I functional

200 categories (Figure 3b), indicative of a loss in genes associated with the production of fatty acids,
201 phospholipids, and peptidoglycan [28]. Within this group, epibiotic predators have even lower
202 numbers of M and I COGs and some of the smallest genomes. With high GC content and a larger
203 genome, the cooperative predator *Myxococcus xanthus* differs from other predatory bacteria
204 (Figure 3).

205

206 **Periplasmic and epibiotic *Pseudobdellovibrionaceae* vary in gene content**

207 In the comparative genomic analysis of all 21 *Pseudobdellovibrionaceae* strains, between
208 2616 and 3754 genes were annotated per strain, and 95.7% of genes were identified as belonging
209 to 5897 orthogroups (Table S4, Figure 4a). Genome characteristics of novel strains and type
210 strains are shown in Table 2. A total of 142 of these orthogroups (made up of 354 genes) were
211 exclusive to a single strain. A total of 1360 core orthogroups were found in all genomes.

212 Excluding these core orthogroups, *B. qaytius* and *B. gaculeatus* strain SBM16 had the greatest
213 number of unique, shared orthogroups (271). *B. krueschi* strain MYbb4 had the greatest number
214 of strain-specific orthogroups (63) comprising 3.9% of total genes, followed by *B. daniorerio*
215 strain ZFWA1 with 17 strain-specific orthogroups (Table 2). *P. exovorius* JSS had the greatest
216 number of exclusively absent orthogroups (i.e. found in all genomes but *P. exovorius* JSS) (64),
217 followed by *B. daniorerio* strain ZFWA1 with 31 exclusively absent orthogroups.

218 Epibiotic strains shared 102 unique orthogroups that had a higher relative frequency of
219 genes involved in the transport and metabolism of amino acids, nucleotides, coenzymes, and
220 lipids as well as in secondary metabolite biosynthesis, intracellular trafficking, secretion, and
221 vesicular transport (Figure S3). Orthogroup eggNOG-mapper annotations are listed in Table S5.
222 Epibiotic predators also exclusively encoded some of the genes involved in folate biosynthesis
223 (including *folB*, *folP*, and *folC*), as well as ABC transporters of substrates across the cytoplasmic
224 membrane (including *dppB*), synthesis of glutamate (*glnN*) and purine (*purK*), and disposal of

225 toxic ammonia (*rocF*). Orthogroups unique to periplasmic predators (168) had a higher relative
226 frequency of genes involved in numerous COG categories including transcription, replication,
227 recombination and repair, cell wall biogenesis, cell motility, and signal transduction mechanisms
228 (Figure S3). Here, unique genes included genes encoding histidine kinases and genes involved in
229 chemotaxis.

230 The distribution of several peptidoglycan-modifying enzymes differs between predation
231 strategies. While all *Pseudobdellovibrionaceae* encode a housekeeping penicillin binding protein
232 (*dacB*) involved in cell wall integrity, periplasmic predators exclusively share an *mltA*-like lytic
233 transglycosylase (Bd3285) and a *slt* lytic transglycosylase (Bd1124) (Figure 4b). Epibiotic
234 strains encode two peptidoglycan modifying enzymes that were absent from periplasmic strains
235 (Figure 4b). These include anhydro-N-acetylmuramic acid kinase (anmK) and a polysaccharide
236 deacetylase involved in cell wall recycling and peptidoglycan remodeling, respectively.

237

238 **Many *Pseudobdellovibrionaceae* lack genes involved in host independence**

239 Genomes of the epibiotic predators and *Bdellovibrio bagaluti* strains MYbb7 and
240 MYbb10, as well as *Bdellovibrio* sp. ZAP7 and KM01, lack the *hit* locus gene Bd0108 (Figure
241 4b). A similar pattern was observed for the LysR family transcriptional regulator gene Bd3229.
242 However, this gene was also absent in *B. bacteriovorus* W.

243 Further, epibiotic predators and *Bdellovibrio daniorerio* strain ZFWA1 lack the genes
244 *motAB1* (Bd0144, Bd0145) and *motAB2* (Bd3021, Bd3020 except for SBM16), and a histidine
245 kinase (Bd3126), which are genes previously reported to be involved in host independence (HI;
246 i.e., prey-independent feeding, see discussion). In contrast, two other putative HI genes, *rhlB*
247 (Bd3461) and *pcnB* (Bd3464), as well as *motAB3* (Bd3254 and Bd3253) were present in all
248 strains. Additionally, the described HI-related histidine kinase Bd3650/Bd1535/Bd2843 was
249 absent in all these strains, and also in MYbb1 and *B. bacteriovorus* W. Two other histidine

250 kinase genes (Bd3393 and Bd2335) and Bd2152 (a glycerol-3-phosphate transporter [29]) were
251 exclusively absent in epibiotic predators. Additionally, epibiotic predators and ZFWA1
252 exclusively share 12 orthologous genes with annotated functions involved in initial binding of
253 peptides in periplasmic space (*dppA*) for ABC-type transport, methionine salvage (*mtnA* and
254 *mtnP*), cell wall formation (*murB*), and tyrosine metabolism (*hgo*).

255

256 ***Pseudobdellovibrionaceae* strains show indications of habitat specificity**

257 We found ASVs matching the 16S rDNA of our newly isolated strains in host-
258 microbiome datasets of zebrafish, stickleback, and worms (Table 3). Interestingly, zebrafish
259 microbiomes only contained *Pseudobdellovibrionaceae* ASVs matching strains that had been
260 isolated from aquatic habitats. In contrast, stickleback microbiomes contained a more diverse set
261 of *Pseudobdellovibrionaceae*, including strains that had been isolated from the direct
262 environment of zebrafish (ZFW), stickleback (SBM), and worms (MYbbs), and were present in
263 up to 80% of samples. Lastly, worm microbiomes rarely contained *Pseudobdellovibrionaceae*
264 ASVs (3% of samples) and did not harbor *Pseudobdellovibrionaceae* ASVs associated with
265 zebrafish or stickleback. However, they did contain *Pseudobdellovibrionaceae* ASVs that had
266 been previously associated with aquatic habitats, although most of the *Pseudobdellovibrionaceae*
267 ASVs belonged to strains isolated from worm-associated environments or other terrestrial
268 habitats.

269

270 **Discussion**

271 *Bdellovibrio* and like organisms (BALOs) play an important role in microbial
272 communities [30–32] and there is growing interest in using BALOs to manipulate microbial
273 communities, especially within host organisms [33–35]. To broaden our understanding of BALO
274 diversity, especially those associated with animal hosts, we isolated nine novel

275 *Pseudobdellovibrionaceae* strains from the environments of three important model animals: the
276 zebrafish, threespine stickleback fish, and the nematode *C. elegans*. We characterized these
277 strains using TEM, comparative genomics and phylogenetic analysis. Two of these nine strains
278 were sufficiently diverged genetically to be considered new genera, including only the third
279 *Pseudobdellovibrionaceae* strain known to use an epibiotic predation strategy, while six strains
280 can be grouped into five new species within the genus *Bdellovibrio*. Our phylogenetic analysis
281 indicates that there are two clades within the family *Pseudobdellovibrionaceae*, separating
282 periplasmic from epibiotic genera (Figure 2b). These novel isolates significantly expand our
283 understanding of BALO biology, especially the genetics and evolution of predation strategies.

284

285 **Epibiotic predation is a derived trait among BALOs**

286 Phylogenetic analysis of our novel isolates allowed us to better understand the evolution
287 of predation modes among BALO species. Bacterial predation is not a monophyletic trait, and
288 predatory bacteria are found in other bacterial phyla. When including other bacterial phyla in the
289 broader phylogeny (Figure 2a), we identified a single clade that contained all periplasmic BALO
290 genera, suggesting that periplasmic predation may be the ancestral phenotype. In contrast,
291 epibiotic BALO genera are dispersed amongst non-predators and periplasmic predators alike,
292 suggesting that epibiotic predation arose in multiple independent lineages. This evolutionary
293 hypothesis differs from that of Deeg et al. [16], who proposed that epibiotic predation is
294 ancestral and periplasmic predation the derived state within the *Pseudobdellovibrionaceae*.
295 However, Deeg et al. [16] used a single gene (16S rRNA) to infer their phylogeny, while we
296 used a set of over 250 single-copy core genes.

297 Our comparative genomic analyses provided additional support for our hypothesis that
298 periplasmic predation is ancestral. Pasternak et al. [14] noted genome reduction in periplasmic
299 predators driven by the dependence on prey amino acids and vitamins as is observed in host-

300 dependent bacteria [36]. If periplasmic predation is ancestral, derived epibiotic predators
301 therefore would exhibit a secondary phase of genome streamlining as first hypothesized by
302 Pasternak et al. [15]. In the present study, epibiotic *Pseudobdellovibrionaceae* genomes show
303 signs of genome degradation, similar to what has been shown for host-associated symbionts [28].
304 This includes higher AT content and coding density, smaller genome size, including fewer DNA
305 repair genes and fewer genes involved in cell envelope biosynthesis and morphology when
306 compared to non-predators (Figure 3 and Figure S3). However, we can base this interpretation
307 only on observations of the three epibiotic *Pseudobdellovibrionaceae* strains described so far.
308 However, this streamlining of epibiotic predators seems to be restricted to
309 *Pseudobdellovibrionaceae* species as periplasmic BALOs in the family *Bacteriovoraceae*
310 including *Halobacteriovorax marinus*, *Bacteriovorax stolpii*, and *Peredibactor starii* had low
311 GC content and high coding density comparable to epibiotic *Pseudobdellovibrionaceae*.
312 Likewise, epibiotic BALOs *Micavibrio aeruginosavorus* and *Vampirovibrio chlorellavorus* had
313 higher GC content and lower coding density than all *Pseudobdellovibrionaceae* predators
314 (Figure 3b).

315

316 **The evolution of epibiotic predation may have involved the loss of “host independence”** 317 **genes**

318 Our comparative genomic analysis identified multiple genes that may have been lost in
319 epibiotic predators during their evolution from a periplasmic ancestor. Many of these are genes
320 involved in “host independence” in *Bdellovibrio bacteriovorus* (Figure 4b), a prey-independent
321 feeding strategy that may be induced under limited prey conditions in nature and on protein-rich
322 media in the laboratory [6, 37] and is caused by a mutation in any of a number of genes. We
323 identified multiple genes associated with host independence (specifically, but not exclusively
324 Type I host independence; [38–43]), including Bd3126 (a histidine kinase), and one of the three

325 motAB gene clusters, Bd0144/Bd0145 (*motABI*), that were absent in the epibiotic
326 *Pseudobdellovibrionaceae* species and their closest relative that used periplasmic predation
327 (*Bdellovenatio daniorerio* ZFWA1), but were present in other periplasmic predators (Figure 4b).

328

329 **Functional differences in peptidoglycan modification differentiate predation strategies**

330 Our comparative analyses provided novel information regarding the biochemistry
331 underlying different predation strategies and builds upon previous studies [15, 18]. Epibiotic
332 genomes lack some peptidoglycan modifying enzymes that have been shown to be important in
333 periplasmic predation (Figure 4B; [16]). Assuming periplasmic predation as the ancestral state,
334 this likely represents a gene loss for epibiotic predators. All *Pseudobdellovibrionaceae* strains
335 encode *dacB*, a housekeeping PBP4 (penicillin binding protein) likely involved in the
336 maintenance of the predator's own cell wall [44]. Periplasmic *Bdellovibrio* predators in the clade
337 that contains both strains HD100 and MYbb1 (Table 2a) all possess a suite of enzymes involved
338 in the modification of the prey cell wall. For example, two *dacB*-like genes, Bd0816 and
339 Bd3459, involved in prey cell rounding to form an osmotically stable bdelloplast and reducing
340 the rate of secondary invasions [44], were absent from some more diverged periplasmic strains
341 and all epibiotic strains. The rate of wasteful secondary invasions may be higher in strains that
342 lack these genes, but this is currently unknown. Similarly, L,D-transpeptidases, Bd0886 and
343 Bd1176, strengthen the prey bdelloplast wall to resist bursting during predator growth within the
344 prey cell [45]. While absent from various strains, an ortholog of these genes is encoded in *B.*
345 *gaculeatus* strain SBM16. Since bdelloplast formation is not necessary for epibiotic predators,
346 these genes may perform a different role in SBM16 or may be fated for removal in further
347 genome streamlining. Interestingly, all four genes involved in bdelloplast integrity were absent
348 from *B. krueschi* strain MYbb4. This, together with the abundance of exclusively present
349 orthogroups (Table 2) may reflect MYbb4's evolved specificity to predate *Ochrobactrum*,

350 although host range was not exhaustively examined here. Further, the diversity, distribution, and
351 function of predatory peptidoglycan-modifying genes is likely influenced by structural and
352 biochemical properties of the prey cell wall such as cross-link chemistry [45], bacterial capsules,
353 surface layers, or acetylation state [46].

354 Notably, an *mltA*-like lytic transglycosylase is exclusive to periplasmic predators. In
355 *Bdellovibrio bacteriovorus* strain HD100, this protein is secreted into the prey periplasm and
356 cleaves the peptidoglycan septum of dividing prey, facilitating the conversion of actively
357 dividing prey into a single spherical bdelloplast [47]. All strains contain an LD carboxypeptidase
358 involved in predator cell wall curvature which causes the formation of a vibrioid and facilitates
359 efficient intracellular growth of HD100 in a spherical prey niche [48]. What role this plays in
360 epibiotic strains is yet to be determined. Most periplasmic predators and *P. exovorus* strain JSS
361 encode peptidoglycan deacetylases (Bd0468 and Bd 3279 or orthologs) that deacetylate the
362 peptidoglycan of the prey [49]. This allows the predator to differentiate between the cell wall of
363 the prey and that of the predator itself with the enzyme *dsIA* (Bd0314) which cuts peptidoglycan
364 depending on acetylation state and functions as an exit enzyme by destroying the prey cell wall
365 [50]. Strains MYbb4, ZFWA1, and JSS all lack *dsIA*, suggesting that MYbb4 and ZFWA1
366 possess an alternative exit strategy.

367 Epibiotic *Pseudobdellovibrionaceae* strains exclusively share *anmK*, which encodes a
368 bifunctional glycosidase/kinase involved in recycling of cell-wall derived anhydroMurNAc [51].
369 Interestingly, all non-*Pseudobdellovibrionaceae* epibiotic predators also encode AnmK as do
370 non-predator relatives (*A. capsulatum*, *V. chlorellavorus*, *M. aeruginosavorus*, *E. adhaerens*, and
371 *S. maltophilia*). While not present in periplasmic predators, this widely conserved gene may be
372 integral to epibiotic predation. Cell-wall recycling through MurNAc dissimilation is a pathway
373 by which bacteria can utilize peptidoglycan fragments from the environment or from the
374 endogenous cell wall [51]. This could be advantageous for predatory bacteria to scavenge prey

375 cell wall material [52]. However, *murQ* is also necessary for anhydroMurNAc recycling, but is
376 absent in *Pseudobdellovibrionaceae* strains. Both *anmK* and *murQ* are present in epibiotic
377 predators *M. aeruginosavorus* and *V. chlorellavorus* as well as *E. adhaerens*. While some
378 epibiotic predators may be able to utilize prey cell wall material through this process, the role
379 and exclusivity of *anmK* in epibiotic *Pseudobdellovibrionaceae* is yet to be uncovered.

380

381 **The family *Pseudobdellovibrionaceae* is more genus and species rich than previously**
382 **thought**

383 Using ANI, we identified new *Pseudobdellovibrionaceae* strains belonging to five new
384 species and two new genera. Further, existing strains proposed to belong to *B. bacteriovorus*
385 likely represent separate species. Renaming these strains as distinct species would enhance our
386 understanding of *Pseudobdellovibrionaceae* diversity and evolution.

387 Targeting few environments in relation to host organisms of interest was enough to isolate novel
388 BALOs. Thus, true BALO species diversity is largely underexplored. This may be particularly
389 true for difficult to culture species such as epibiotic predators. In general, epibiotic predators
390 have a narrower prey range than periplasmic predators and produce fewer offspring per prey cell,
391 resulting in lower population growth rates [13, 16, 17], a pattern we also observed for our novel
392 epibiotic isolate *B. gaculeatus* strain SBM16.

393

394 ***Pseudobdellovibrionaceae* are likely widespread among host microbiomes**

395 Although there is growing interest in using BALOs to manipulate host-associated
396 microbiomes, there have been very few studies that have attempted to isolate host-associated
397 BALO species [53–57]. By sampling the immediate environment of three model animal hosts
398 (zebrafish, threespine stickleback, and *C. elegans*) we successfully isolated new
399 *Pseudobdellovibrionaceae* and detected ASVs (highly) similar to the 16S rDNA sequences of

400 those strains in microbiomes of the hosts: *Bdellovenatio daniorerio* strain ZFWA1 ASVs were
401 found in zebrafish eggs and larvae, as well as in samples of threespine stickleback guts (Table 3).
402 Zebrafish microbiomes exclusively contained *Pseudobdellovibrionaceae* ASVs of strains
403 originally isolated from aquatic environments. In contrast, stickleback microbiomes contained
404 *Pseudobdellovibrionaceae* ASVs of species originally isolated from many different
405 environments (Table 3), including two *Bdellovibrio* species that we isolated from compost (*B.*
406 *tomkyle* strain MYbb1 and *B. krueschi* strain MYbb4). Interestingly, ASVs of *B. krueschi* strain
407 MYbb4 were highly prevalent across stickleback gut samples. MYbb4 specifically preys on
408 *Ochrobactrum*, and we indeed detected *Ochrobactrum* ASVs in these same stickleback samples.
409 We found ASVs of aquatic *Pseudobdellovibrionaceae* in worm microbiomes (Table 3). One
410 example is the Tiberius strain, isolated from the nutrient-rich Tiber River in Italy. This strain
411 belongs to the same species as *B. tiberii* MYbb2, which we isolated from compost material in
412 Kiel, Germany. This indicates that the same *Bdellovibrio* strain can be found in multiple habitats
413 and suggests that habitat preferences may depend more on the presence of suitable prey than on
414 the habitat itself.

415 The prey preferences of different *Pseudobdellovibrionaceae* species likely influences
416 their distributions. For example, *B. daniorerio* strain ZFWA1 was isolated using *Aeromonas*
417 *veronii*, and this genus is commonly found associated with fish as well as in free-living aquatic
418 microbiomes. We observed ASVs of *B. daniorerio* in zebrafish and stickleback microbiomes,
419 which also contained *Aeromonas* species. Similarly, most of our compost (MYbb) isolates were
420 isolated using *E. coli* as prey. *E. coli* strains are widespread across different environments, and
421 indeed we find many *Pseudobdellovibrionaceae* ASVs in microbiomes from both worms and
422 stickleback fish. In contrast, ASVs of *B. gaculeatus* strain SBM16 were exclusively present in
423 stickleback microbiomes. This species was isolated from a stickleback aquaculture facility, a
424 moderately saline environment. We observed that this species had higher population growth rates

425 in the laboratory when a saline medium was used. However, further research is needed to
426 confirm whether this strain truly exhibits strong habitat specificity toward saltwater.
427 Interestingly, this strain had a distinct flagellum morphology compared to the other isolates (i.e.,
428 smaller wave amplitudes), which may have functional implications in saline environments. In
429 *Shewanella*, a smaller wave amplitude led to decreased spreading in soft agar (consistent with
430 our observation that SBM16 does not grow well on double-layer agar plates) but increased
431 velocity at higher viscosity (as in salt water) [58], a phenomenon observed in other bacteria as
432 well [59].

433 Isolating several new *Pseudobdellovibrionaceae* strains, including an epibiotic BALO,
434 revealed that the diversity within the family is highly underestimated and helped improve
435 genome-based predictions regarding predation mode and its evolutionary origin. Efforts in
436 isolating and sequencing new predatory bacteria will further enhance our knowledge and allow
437 for the testing and application of these strains as alternative probiotics or antibiotics in the future.

438

439 Formal description of five new species and two new genera within the

440 *Pseudobdellovibrionaceae*

441

442 *Bdellovibrio tiberii* sp. nov. (/ti'be:ri.i:/, derived from the name of the river Tiber, from which
443 the first strain was isolated) with type strain MYbb2^T

444 Highly motile cells of vibrioid shape ($0.25 \pm 0.04 \mu\text{m}^2$ in size) with a single flagellum ($3.34 \pm$

445 $0.36 \mu\text{m}$ in length) and a periplasmic predation strategy. The type strain was isolated from *C.*

446 *elegans*-associated compost material, collected from the Kiel Botanical Garden using

447 *Escherichia coli* ML35 as prey. Cells grow on prey lawns as plaques at 28°C.

448 The species belongs to the genus *Bdellovibrio* (within the family *Pseudobdellovibrionaceae*).

449 The genome has a G+C content of 49.8% and is approximately 4.05 Mb in size. The strain is

450 accessible at the DSMZ () and the ATCC ().

451

452 *Bdellovibrio kumpostii* sp. nov. (/kum'pɔs.ti.i:/, latinized from the German word Kompost

453 describing the isolation source, a compost heap in Kiel, Germany) with type strain MYbb5^T

454 Highly motile cells of vibrioid shape ($0.21 \pm 0.03 \mu\text{m}^2$ in size) with a single flagellum ($3.02 \pm$

455 $0.55 \mu\text{m}$ in length) and a periplasmic predation strategy. The type strain was isolated from *C.*

456 *elegans*-associated compost material, collected from the Kiel Botanical Garden using

457 *Escherichia coli* ML35 as prey. Cells grow on prey lawns as plaques at 28°C.

458 The species belongs to the genus *Bdellovibrio* (within the family *Pseudobdellovibrionaceae*).

459 The genome has a G+C content of 49.9% and is approximately 3.89 Mb in size. The strain is

460 accessible at the DSMZ () and the ATCC ().

461

462 *Bdellovibrio tomkyle* sp. nov. (/tɔm'ki.le/, derived from the Low German binomial tom kyle

463 referring to the old name for the city of Kiel in Germany, meaning tom “at the” kyle “fjord”, as

464 the strain was isolated in Kiel) with type strain MYbb1^T

465 Highly motile cells of vibrioid shape ($0.19 \pm 0.02 \mu\text{m}^2$ in size) with a single flagellum ($3.02 \pm$

466 $0.22 \mu\text{m}$ in length) and a periplasmic predation strategy. The type strain was isolated from *C.*

467 *elegans*-associated compost material, collected from the Kiel Botanical Garden using

468 *Escherichia coli* ML35 as prey. Cells grow on prey lawns as plaques at 28°C.

469 The species belongs to the genus *Bdellovibrio* (within the family *Pseudobdellovibrionaceae*).

470 The genome has a G+C content of 48.8% and is approximately 3.88 Mb in size. The strain is

471 accessible at the DSMZ () and the ATCC ().

472

473 *Bdellovibrio bagaluti* sp. nov. (/baga'lu:ti/, derived from the Low German word Bagalut,
474 referring to someone who is mischievous or unruly to reflect the predatory nature of the strain)
475 with type strain MYbb7^T
476 Highly motile cells of vibrioid shape ($0.21 \pm 0.03 \mu\text{m}^2$ in size) with a single flagellum ($2.99 \pm$
477 $0.44 \mu\text{m}$ in length) and a periplasmic predation strategy. The type strain was isolated from *C.*
478 *elegans*-associated compost material, collected from the Kiel Botanical Garden using
479 *Escherichia coli* ML35 as prey. Cells grow on prey lawns as plaques at 28°C.
480 The species belongs to the genus *Bdellovibrio* (within the family *Pseudobdellovibrionaceae*).
481 The genome has a G+C content of 45% and is approximately 3.8 Mb in size. The strain is
482 accessible at the DSMZ () and the ATCC ().

483

484 *Bdellovibrio krueschi* sp. nov. (/ˈkrʏʃi/, derived from the Low German word krüsch which
485 describes someone who is picky reflecting the small prey range of the species) with type strain
486 MYbb4^T
487 Highly motile cells of vibrioid shape ($0.25 \pm 0.03 \mu\text{m}^2$ in size) with a single flagellum ($2.58 \pm$
488 $0.33 \mu\text{m}$ in length) and a periplasmic predation strategy. The type strain was isolated from *C.*
489 *elegans*-associated compost material, collected from the Kiel Botanical Garden using
490 *Ochrobactrum* MYb71 as prey. Cells grow on prey lawns as plaques at 28°C. So far, only
491 members of the genus *Ochrobactrum* have been identified as prey.
492 The species belongs to the genus *Bdellovibrio* (within the family *Pseudobdellovibrionaceae*).
493 The genome has a G+C content of 45.2% and is approximately 3.52 Mb in size. The strain is
494 accessible at the DSMZ () and the ATCC ().

495

496 *Bdellovenatio* gen nov. (/bdelouva'neifi,ou/, derived from Latin *bdella* meaning “leech” and
497 *venatio* meaning “hunting”, referring to the rapid movement of the cells) with type species

498 *daniorerio* sp. nov. (/dæniɔ:'rɛriou/, derived from the Latin binomial *Danio rerio*, the scientific
499 name of the zebrafish in which this bacterium has been found) and type strain ZFWA1^T
500 Highly motile cells of vibrioid shape ($0.25 \pm 0.05 \mu\text{m}^2$) with a single flagellum ($2.77 \pm 0.25 \mu\text{m}$
501 in length) and a periplasmic predation strategy. The type strain was isolated from water collected
502 at the University of Oregon zebrafish aquaculture facility on the campus in Eugene, Oregon,
503 USA, using *Aeromonas veronii* ZOR0001 as prey. Cells grow on prey lawns as plaques at 28°C.
504 The species belongs to a unique genus in the family *Pseudobdellovibrionaceae*. The genome of
505 has a G+C content of 42.9% and is approximately 3.21 Mb in size. The strain is accessible at the
506 DSMZ () and the ATCC ().

507
508 *Bdellovampiro* gen nov. (/bdɛlou'væmpiroʊ/, derived from Latin *bdella* meaning “leech” and
509 *vampiro* meaning “vampire” referring to its epibiotic predation strategy) with type species
510 *gaculeatus* sp. nov. (/gɑ:kju:'li:ətəs/, a contraction of the Latin binomial *Gasterosteus aculeatus*,
511 the scientific name of the threespine stickleback fish in which this bacterium has been found) and
512 type strain SBM16^T
513 Highly motile cells of elongated vibrioid shape ($0.77 \pm 0.24 \mu\text{m}^2$) with a thin and very long (7.13
514 $\pm 1.57 \mu\text{m}$) single flagellum and an epibiotic predation strategy. The type strain was isolated
515 from water collected at the University of Oregon threespine stickleback aquaculture facility on
516 the campus in Eugene, Oregon, USA, using *Escherichia coli* ML35 as prey. Cells grow together
517 with prey at 20°C. This strain is mesohalophilic, growing optimally in media amended with 2
518 g/L sea salt. The species belongs to a unique genus in the family *Pseudobdellovibrionaceae*. The
519 genome has a G+C content of 43.5% and is approximately 3.08 Mb in size. The strain is
520 accessible at the DSMZ () and the ATCC ().

521

522 **Acknowledgements**

523 We thank the Bohannan and Schulenburg groups for discussions and advice on this work. For
524 genomic sequencing, we further thank the Competence Centre for Genomic Analysis (CCGA)
525 Kiel. For obtaining environmental samples, we thank the Botanical Garden in Kiel, Germany, the
526 Cresko Stickleback Facility, and the University of Oregon Zebrafish Facility. We are grateful for
527 funding from the German Science Foundation (Deutsche Forschungsgemeinschaft, DFG) within
528 the Collaborative Research Center (CRC) 1182 on the Origin and Function of Metaorganisms
529 (Project-ID 261376515 – SFB 1182, project A4.3 to HS), individual DFG project JO 1786/1-1
530 (to JJ), the Max-Planck Society (fellowship to HS), the NIH P01-GM125576 to BJMB, and the
531 NIH Research Supplement to Promote Diversity in Health-Related Research to RLM.

532

533 **Competing Interests**

534 The authors declare no competing interests.

535

536 **Data Availability Statement**

537 All raw sequences are available in the SRA under PRJNA1185762 and assembled

538 *Pseudobdellovibrionaceae* genomes are available in the NCBI under PRJNA1185297.

539

540 **References**

- 541 1. Menge BA, Sutherland JP. Species Diversity Gradients: Synthesis of the Roles of Predation,
542 Competition, and Temporal Heterogeneity. *The American Naturalist* 1976; **110**: 351–369.
- 543 2. Baum JK, Worm B. Cascading top-down effects of changing oceanic predator abundances.
544 *Journal of Animal Ecology* 2009; **78**: 699–714.
- 545 3. Welsh RM, Zaneveld JR, Rosales SM, Payet JP, Burkepille DE, Thurber RV. Bacterial predation
546 in a marine host-associated microbiome. *ISME J* 2016; **10**: 1540–1544.
- 547 4. Welsh RM, Rosales SM, Zaneveld JR, Payet JP, McMinds R, Hubbs SL, et al. Alien vs. predator:
548 bacterial challenge alters coral microbiomes unless controlled by *Halobacteriovorax* predators.

- 549 *PeerJ* 2017; **5**: e3315.
- 550 5. Johnke J, Fraune S, Bosch TCG, Hentschel U, Schulenburg H. *Bdellovibrio* and like organisms
551 are predictors of microbiome diversity in distinct host groups. *Microb Ecol* 2020; **79**: 252–257.
- 552 6. Stolp H, Starr MP. *Bdellovibrio bacteriovorus* gen. et sp. n., a predatory, ectoparasitic, and
553 bacteriolytic microorganism. *Antonie van Leeuwenhoek* 1963; **29**: 217–248.
- 554 7. Ezzedine JA, Desdevises Y, Jacquet S. *Bdellovibrio* and like organisms: current understanding
555 and knowledge gaps of the smallest cellular hunters of the microbial world. *Critical Reviews in*
556 *Microbiology* 2022; **48**: 428–449.
- 557 8. Lai TF, Ford RM, Huwiler SG. Advances in cellular and molecular predatory biology of
558 *Bdellovibrio bacteriovorus* six decades after discovery. *Front Microbiol* 2023; **14**.
- 559 9. Williams HN, Lymperopoulou DS, Athar R, Chauhan A, Dickerson TL, Chen H, et al.
560 *Halobacteriovorax*, an underestimated predator on bacteria: potential impact relative to viruses
561 on bacterial mortality. *ISME J* 2016; **10**: 491–499.
- 562 10. Snyder AR. 16S rDNA sequence analysis of environmental *Bdellovibrio*-and-like organisms
563 (BALO) reveals extensive diversity. *International Journal of Systematic and Evolutionary*
564 *Microbiology* 2002; **52**: 2089–2094.
- 565 11. Göker M. Filling the gaps: missing taxon names at the ranks of class, order and family.
566 *International Journal of Systematic and Evolutionary Microbiology* 2022; **72**.
- 567 12. Waite DW, Chuvochina M, Pelikan C, Parks DH, Yilmaz P, Wagner M, et al. Proposal to
568 reclassify the proteobacterial classes Deltaproteobacteria and Oligoflexia, and the phylum
569 Thermodesulfobacteria into four phyla reflecting major functional capabilities. *International*
570 *Journal of Systematic and Evolutionary Microbiology* 2020; **70**: 5972–6016.
- 571 13. Santin YG, Sogues A, Bourigault Y, Remaut HK, Laloux G. Lifecycle of a predatory bacterium
572 vampirizing its prey through the cell envelope and S-layer. *Nat Commun* 2024; **15**: 3590.
- 573 14. Pasternak Z, Pietrokovski S, Rotem O, Gophna U, Lurie-Weinberger MN, Jurkevitch E. By their
574 genes ye shall know them: genomic signatures of predatory bacteria. *ISME J* 2013; **7**: 756–769.
- 575 15. Pasternak Z, Njagi M, Shani Y, Chanyi R, Rotem O, Lurie-Weinberger MN, et al. In and out: an
576 analysis of epibiotic vs periplasmic bacterial predators. *ISME J* 2014; **8**: 625–635.

- 577 16. Deeg CM, Le TT, Zimmer MM, Suttle CA. From the inside out: an Epibiotic *Bdellovibrio*
578 predator with an expanded genomic complement. *J Bacteriol* 2020; **202**.
- 579 17. Koval SF, Hynes SH, Flannagan RS, Pasternak Z, Davidov Y, Jurkevitch E. *Bdellovibrio*
580 *exovor* sp. nov., a novel predator of *Caulobacter crescentus*. *International Journal of*
581 *Systematic and Evolutionary Microbiology* 2013; **63**: 146–151.
- 582 18. Davis SC, Cerra J, Williams LE. Comparative genomics of obligate predatory bacteria belonging
583 to phylum Bdellovibrionota highlights distribution and predicted functions of lineage-specific
584 protein families. *mSphere* 2024; **9**: e00680-24.
- 585 19. Thomashow LS, Rittenberg SC. Isolation and composition of sheathed flagella from *Bdellovibrio*
586 *bacteriovorus* 109J. *J Bacteriol* 1985; **163**: 1047–1054.
- 587 20. Kaplan M, Chang Y-W, Oikonomou CM, Nicolas WJ, Jewett AI, Kreida S, et al. *Bdellovibrio*
588 predation cycle characterized at nanometre-scale resolution with cryo-electron tomography. *Nat*
589 *Microbiol* 2023; 1–13.
- 590 21. Lambert C, Evans KJ, Till R, Hobley L, Capeness M, Rendulic S, et al. Characterizing the
591 flagellar filament and the role of motility in bacterial prey-penetration by *Bdellovibrio*
592 *bacteriovorus*. *Mol Microbiol* 2006; **60**: 274–286.
- 593 22. Iida Y, Hobley L, Lambert C, Fenton AK, Sockett RE, Aizawa S-I. Roles of Multiple Flagellins
594 in Flagellar Formation and Flagellar Growth Post Bdelloplast Lysis in *Bdellovibrio*
595 *bacteriovorus*. *Journal of Molecular Biology* 2009; **394**: 1011–1021.
- 596 23. Thomashow LS, Rittenberg SC. Waveform analysis and structure of flagella and basal complexes
597 from *Bdellovibrio bacteriovorus* 109J. *J Bacteriol* 1985; **163**: 1038–1046.
- 598 24. Fenton AK, Kanna M, Woods RD, Aizawa S-I, Sockett RE. Shadowing the actions of a predator:
599 Backlit fluorescent microscopy reveals synchronous nonbinary septation of predatory
600 *Bdellovibrio* inside prey and exit through discrete bdelloplast pores. *Journal of Bacteriology*
601 2010; **192**: 6329–6335.
- 602 25. Jain C, Rodriguez-R LM, Phillippy AM, Konstantinidis KT, Aluru S. High throughput ANI
603 analysis of 90K prokaryotic genomes reveals clear species boundaries. *Nature Communications*
604 2018; **9**: 5114.

- 605 26. Konstantinidis KT, Rosselló-Móra R, Amann R. Uncultivated microbes in need of their own
606 taxonomy. *ISME J* 2017; **11**: 2399–2406.
- 607 27. Rodriguez-R LM, Conrad RE, Viver T, Feistel DJ, Lindner BG, Venter SN, et al. An ANI gap
608 within bacterial species that advances the definitions of intra-species units. *mBio* 2023; **15**:
609 e02696-23.
- 610 28. McCutcheon JP, Moran NA. Extreme genome reduction in symbiotic bacteria. *Nature Reviews*
611 *Microbiology* 2012; **10**: 13–26.
- 612 29. Karunker I, Rotem O, Dori-Bachash M, Jurkevitch E, Sorek R. A global transcriptional switch
613 between the attack and growth forms of *Bdellovibrio bacteriovorus*. *PLOS ONE* 2013; **8**: e61850.
- 614 30. Inoue D, Nakamura S, Sugiyama T, Ike M. Potential of predatory bacteria to colonize the
615 duckweed microbiome and change its structure: A model study using the obligate predatory
616 bacterium, *Bacteriovorax* sp. HI3. *Microbes and Environments* 2023; **38**.
- 617 31. Chen H, Young S, Berhane T-K, Williams HN. Predatory *Bacteriovorax* communities ordered by
618 various prey species. *PLOS ONE* 2012; **7**: e34174.
- 619 32. Chen H, Laws EA, Martin JL, Berhane T-K, Gulig PA, Williams HN. Relative contributions of
620 *Halobacteriovorax* and bacteriophage to bacterial cell death under various environmental
621 conditions. *mBio* 2018; **9**: 10.1128/mbio.01202-18.
- 622 33. Cavallo FM, Jordana L, Friedrich AW, Glasner C, van Dijk JM. *Bdellovibrio bacteriovorus*: a
623 potential ‘living antibiotic’ to control bacterial pathogens. *Critical Reviews in Microbiology*
624 2021; **47**: 630–646.
- 625 34. Bonfiglio G, Neroni B, Radocchia G, Marazzato M, Pantanella F, Schippa S. Insight into the
626 possible use of the predator *Bdellovibrio bacteriovorus* as a probiotic. *Nutrients* 2020; **12**: 2252.
- 627 35. Dwidar M, Monnappa AK, Mitchell RJ. The dual probiotic and antibiotic nature of *Bdellovibrio*
628 *bacteriovorus*. *BMB Rep* 2012; **45**: 71–78.
- 629 36. Klasson L, Andersson SGE. Evolution of minimal-gene-sets in host-dependent bacteria. *Trends*
630 *in Microbiology* 2004; **12**: 37–43.
- 631 37. Shilo M, Bruff B. Lysis of Gram-negative bacteria by host-independent ectoparasitic *Bdellovibrio*
632 *bacteriovorus* isolates. *Journal of General Microbiology* 1965; **40**: 317–328.

- 633 38. Medina AA, Shanks RM, Kadouri DE. Development of a novel system for isolating genes
634 involved in predator-prey interactions using host independent derivatives of *Bdellovibrio*
635 *bacteriovorus* 109J. *BMC Microbiology* 2008; **8**: 33.
- 636 39. Cotter TW, Thomashow MF. Identification of a *Bdellovibrio bacteriovorus* genetic locus, hit,
637 associated with the host-independent phenotype. *Journal of Bacteriology* 1992; **174**: 6018–6024.
- 638 40. Wurtzel O, Dori-Bachash M, Pietrokovski S, Jurkevitch E, Sorek R. Mutation detection with
639 next-generation resequencing through a mediator genome. *PLOS ONE* 2010; **5**: e15628.
- 640 41. Roschanski N, Klages S, Reinhardt R, Linscheid M, Strauch E. Identification of genes essential
641 for prey-independent growth of *Bdellovibrio bacteriovorus* HD100. *Journal of Bacteriology*
642 2011; **193**: 1745–1756.
- 643 42. Capeness MJ, Lambert C, Lovering AL, Till R, Uchida K, Chaudhuri R, et al. Activity of
644 *Bdellovibrio* hit locus proteins, Bd0108 and Bd0109, links type IVa pilus extrusion/retraction
645 status to prey-independent growth signalling. *PLOS ONE* 2013; **8**: e79759.
- 646 43. Mookherjee A, Mitra M, Sason G, Jose PA, Martinenko M, Pietrokovski S, et al. Flagellar stator
647 genes control a trophic shift from obligate to facultative predation and biofilm formation in a
648 bacterial predator. *mBio* 2024; **15**: e00715-24.
- 649 44. Lerner TR, Lovering AL, Bui NK, Uchida K, Aizawa S-I, Vollmer W, et al. Specialized
650 peptidoglycan hydrolases sculpt the intra-bacterial niche of predatory *Bdellovibrio* and increase
651 population fitness. *PLOS Pathogens* 2012; **8**: e1002524.
- 652 45. Kuru E, Lambert C, Rittichier J, Till R, Ducret A, Derouaux A, et al. Fluorescent D-amino-acids
653 reveal bi-cellular cell wall modifications important for *Bdellovibrio bacteriovorus* predation. *Nat*
654 *Microbiol* 2017; **2**: 1648–1657.
- 655 46. Das SK, Negus D. How do Gram-negative bacteria escape predation by *Bdellovibrio*
656 *bacteriovorus*? *npj Antimicrob Resist* 2024; **2**: 1–8.
- 657 47. Banks EJ, Lambert C, Mason SS, Tyson J, Radford PM, McLaughlin C, et al. An MltA-like Lytic
658 transglycosylase secreted by *Bdellovibrio bacteriovorus* cleaves the prey septum during predatory
659 invasion. *J Bacteriol* 2023; **205**: e00475-22.
- 660 48. Banks EJ, Valdivia-Delgado M, Biboy J, Wilson A, Cadby IT, Vollmer W, et al. Asymmetric

- 661 peptidoglycan editing generates cell curvature in *Bdellovibrio predatory* bacteria. *Nat Commun*
662 2022; **13**: 1509.
- 663 49. Lambert C, Lerner TR, Bui NK, Somers H, Aizawa S-I, Liddell S, et al. Interrupting
664 peptidoglycan deacetylation during *Bdellovibrio* predator-prey interaction prevents ultimate
665 destruction of prey wall, liberating bacterial-ghosts. *Sci Rep* 2016; **6**: 26010.
- 666 50. Harding CJ, Huwiler SG, Somers H, Lambert C, Ray LJ, Till R, et al. A lysozyme with altered
667 substrate specificity facilitates prey cell exit by the periplasmic predator *Bdellovibrio*
668 *bacteriovorus*. *Nat Commun* 2020; **11**: 4817.
- 669 51. Jaeger T, Mayer C. N-acetylmuramic acid 6-phosphate lyases (MurNac etherases): role in cell
670 wall metabolism, distribution, structure, and mechanism. *Cell Mol Life Sci* 2008; **65**: 928–939.
- 671 52. Li Q-M, Zhou Y-L, Wei Z-F, Wang Y. Phylogenomic insights into distribution and adaptation of
672 *Bdellovibrionota* in marine waters. *Microorganisms* 2021; **9**: 757.
- 673 53. Xi Y, Pan Y, Li M, Zeng Q, Wang M. Evaluation of the application potential of *Bdellovibrio* sp.
674 YBD-1 isolated from Yak faeces. *Sci Rep* 2024; **14**: 13010.
- 675 54. Chu W-H, Zhu W. Isolation of *Bdellovibrio* as biological therapeutic agents used for the
676 treatment of *Aeromonas hydrophila* infection in fish: *Aeromonas hydrophila* therapeutic
677 *Bdellovibrio*. *Zoonoses and Public Health* 2009; **57**: 258–264.
- 678 55. Cao H, He S, Wang H, Hou S, Lu L, Yang X. *Bdellovibrios*, potential biocontrol bacteria against
679 pathogenic *Aeromonas hydrophila*. *Veterinary Microbiology* 2012; **154**: 413–418.
- 680 56. Schwudke D, Strauch E, Krueger M, Appel B. Taxonomic studies of predatory *Bdellovibrios*
681 based on 16S rRNA analysis, ribotyping and the hit locus and characterization of isolates from
682 the gut of animals. *Systematic and Applied Microbiology* 2001; **24**: 385–394.
- 683 57. Ottaviani D, Pieralisi S, Chierichetti S, Rocchegiani E, Hattab J, Mosca F, et al. *Vibrio*
684 *parahaemolyticus* control in mussels by a *Halobacteriovorax* isolated from the Adriatic sea, Italy.
685 *Food Microbiology* 2020; **92**: 103600.
- 686 58. Kühn MJ, Schmidt FK, Farthing NE, Rossmann FM, Helm B, Wilson LG, et al. Spatial
687 arrangement of several flagellins within bacterial flagella improves motility in different
688 environments. *Nat Commun* 2018; **9**: 5369.

- 689 59. Schneider WR, Doetsch RN. Effect of viscosity on bacterial motility. *J Bacteriol* 1974; **117**: 696–
690 701.
- 691 60. Small CM, Beck EA, Currey MC, Tavalire HF, Bassham S, Cresko WA. Host genomic variation
692 shapes gut microbiome diversity in threespine stickleback fish. *mBio* 2023; **14**: e00219-23.
- 693 61. Small CM, Currey M, Beck EA, Bassham S, Cresko WA. Highly reproducible 16S sequencing
694 facilitates measurement of host genetic influences on the stickleback gut microbiome. *mSystems*
695 2019; **4**: 10.1128/msystems.00331-19.
- 696 62. Johnke J, Dirksen P, Schulenburg H. Community assembly of the native *C. elegans* microbiome
697 is influenced by time, substrate and individual bacterial taxa. *Environmental Microbiology* 2020;
698 **22**: 1265–1279.
- 699 63. Johnke J, Zimmermann J, Stegemann T, Langel D, Franke A, Thingholm L, et al. *Caenorhabditis*
700 nematodes influence microbiome and metabolome characteristics of their natural apple substrates
701 over time. *mSystems* 2025; **0**: e01533-24.

702

703 **Tables**

704 **Table 1. Phenotypic characterization of novel *Pseudobdellovibrionaceae* isolates.** Values are
705 expressed as mean ± standard error (MYbb1, MYbb2, MYbb4, ZFWA1) or as mean ± standard
706 deviation (MYbb5, MYbb7, MYbb10, MYbb11, SBM16). Respective highest/lowest values are
707 highlighted in bold. Measurements for all independent experiments and grids are given in Table
708 S1.

709 ^aSpecies named according to results of comparative genome analysis, see section below for
710 details.

711 ^bThe Feret diameter ratio was used as a proxy for cell size and shape, with higher values
712 indicating elongated cells.

713 ^cPhenotype confirmed by TEM imaging after negative staining.

714 ^dDescription for strains with outstanding phenotype.

715

716 **Table 2. Genome comparison of novel *Pseudobdellovibrionaceae* isolates with *Bdellovibrio***
717 **and *Pseudobdellovibrio* type strains.** Genome quality estimates of % completion (% comp.) and
718 % contamination (% cont.) were obtained from Checkm2. The number of coding genes (CDS)
719 and different types of RNA genes were predicted using Prokka. Exclusively present orthogroups
720 (OG) defined by Orthofinder were only found in a single genome, and exclusively absent
721 orthogroups were found in all genomes but one. Novel isolates are bolded, and type strains are
722 indicated with an asterisk.

723 ^aOther programs reported deviating levels of contamination, including checkm1 (5.41%),
724 BUSCO (3.2%), and NCBI fcs-gx (0%).

725

726 **Table 3: *Pseudobdellovibrionaceae* strains can be found in 16S rDNA data sets of relevant**
727 **hosts.** Number of the different *Pseudobdellovibrionaceae* ASVs with up to 4 mismatches (i.e.
728 99% identity) and their prevalence are shown for each microbiome study and all
729 *Pseudobdellovibrionaceae* strains used in this study.

730 ⁰⁻⁴: number of mismatches to reference sequences

731 ^aSkin and gut samples collected in 2018 from wildtype adult zebrafish (238 days post
732 fertilization or dpf) reared at the University of Oregon Zebrafish Facility under standard
733 husbandry conditions. Unpublished. Sequenced 16S rRNA region: V4.

734 ^bEgg samples from 0, 1, and 2 dpf wildtype zebrafish collected in 2022 at the University of
735 Oregon Zebrafish Facility under standard husbandry conditions. Unpublished. Sequenced 16S
736 rRNA region: V4.

737 ^cEgg (0 and 2 dpf) and larval gut (5 and 7 dpf) samples from wildtype zebrafish collected in
738 2023 at the University of Oregon Zebrafish Facility under standard husbandry conditions.
739 Unpublished. Sequenced 16S rRNA region: V4.

740 ^dGut samples collected in 2016 from juvenile threespine stickleback (60dpf) reared at the Cresko
741 Stickleback facility at the University of Oregon under standard husbandry conditions. Published
742 in [60]. Sequenced 16S rRNA region: V4.

743 ^eGut samples collected in 2015 from adult male threespine stickleback (12-16 months) reared at
744 the Cresko Stickleback facility at the University of Oregon under standard husbandry conditions.
745 Published in [61]. Sequenced 16S rRNA region: V4.

746 ^fNatural worm samples collected from a compost heap in 2016-2017 and published in [62].
747 Sequenced 16S rRNA region: V3-V4.

748 ^gNatural worm samples collected from apples on a compost heap in 2019-2020 and published in
749 [63]. Sequenced 16S rRNA region: V3-V4.

750

751 *multiple ASVs in worm samples matched similarly well to multiple *Pseudobdellovibrionaceae*
752 strains

753

754 **Figure Legends**

755 **Figure 1: Cell shape and predation mode of *Pseudobdellovibrionaceae* strains MYbb2,**

756 **MYbb4, ZFWA1 and SBM16.** Life cycles of periplasmic (purple) and epibiotic (yellow)

757 *Pseudobdellovibrionaceae* isolates are schematically represented on the left. Numbers in image

758 corners correspond to the proposed life cycle stage. The upper panels illustrate periplasmic

759 *Pseudobdellovibrionaceae* isolates. Stage 1 images represent *Pseudobdellovibrionaceae* cells in

760 attack phase. In stage 2, predators are attached to prey cells (p). Stages 4-7 demonstrate intra-

761 periplasmic growth in bdelloplasts (bd), with one or more *Pseudobdellovibrionaceae* cells

762 confined within the outer membrane of a prey cell. Stage 8 depicts *Pseudobdellovibrionaceae*

763 cells leaving the prey ghost cell (gh). The lower panels display the epibiotic *Bdellovampiro*

764 *gaculeatus* strain SBM16. This strain has a long flagellum, as illustrated in stage 1 images with

765 white arrows at the start and end point of the flagellum. After attachment to and penetration of
766 the outer membrane, epibiotic cells grow and divide outside prey cells (stages 4-5) as indicated
767 by different sizes of cells and by septation in elongated bacteria. Samples were imaged by TEM
768 after negative staining. Scale bar is 500 nm. Life cycle images created in BioRender. Wülbern, J.
769 (2024) BioRender.com/t31h353.

770

771 **Figure 2. Phylogenetic relationship between various predatory and non-predatory**
772 **prokaryotes.** IQ-TREE was used to infer phylogenetic trees by maximum likelihood with
773 bootstrap approximation. a) Phylogenetic relationships between selected prokaryotic species
774 based on phylogenomic analysis using 265 single-copy genes found in 82.4% of species
775 predicted by Orthofinder. All branch support values are reported in blue. b) Relationships among
776 *Pseudobdellovibrionaceae* strains based on phylogenomic analysis using 1099 single-copy core
777 genes predicted by Orthofinder. All branch support values from bootstrapping approximation
778 were 100. Novel isolates are bolded and listed by the newly proposed names based on 65% AAI
779 genus and 95% ANI species designations.

780

781 **Figure 3. Relationship between different genome metrics of predatory and non-predatory**
782 **bacteria.** a) Relationship between coding density and GC content. b) Relationship between the
783 total combined number of genes in the M (cell envelope biogenesis, outer membrane) and I (lipid
784 metabolism) clusters of orthologous groups (COG) categories and genome size. All bacterial
785 species in Figure 2b are included.

786

787 **Figure 4. Variation in gene content by predation strategy.** a) The number of shared
788 orthologous genes in *Pseudobdellovibrionaceae* strains identified using Orthofinder. The top 22
789 shared orthologous gene sets are shown. b) Presence of genes involved in peptidoglycan

790 modification and host independence in *Pseudobdellovibrionaceae* isolates. Dark gray cells
791 indicate the presence of the gene with the best protein match listed under seed ortholog. Light
792 gray cells indicate genes with a different seed ortholog that belong in the same orthogroup. The
793 asterisk indicates that only gene Bd3021 is present in SBM16, not Bd3020. All novel isolate
794 names are bolded.

795

796 **Supplementary Tables**

797 **Table S1. Size measurements for *Pseudobdellovibrionaceae* strains described in this study.**

798 Measurements of bacteria were performed on images taken at 11,000x (TIA camera) or 16,500x
799 (MegaView III camera) magnification using FIJI software (Schindelin et al., 2012). A segmented
800 line tool was used to measure the length of flagella, and a polygon tool was used to measure the
801 cell body area, perimeter and Feret diameter. Culture column indicates whether fresh prey was
802 added before imaging or whether standard overnight cultures were used. The mean, standard
803 deviation (SD) and count numbers are displayed for flagellum and cell body measurements.
804 Units for each measurement are indicated in square brackets. Count column refers to the number
805 of images analyzed for mean values. Run column indicates how many independent experiments
806 (the first number) and how many independent grids (the second number) were analyzed for each
807 sample.

808

809 **Table S2. Average Nucleotide Identity (a) and Average Amino Acid Identity (b) between**
810 **strains.** Pairwise ANI was calculated with fastANI v1.34 and pairwise AAI was calculated with
811 CompareM v0.1.2.

812

813 **Table S3. Genbank accession numbers of genome assemblies included in phylogenomic**
814 **analyses.** Prokaryotic genomes were used to infer phylogenetic relationships between

815 periplasmic and epibiotic BALOs. *Pseudobdellovibrionaceae* genomes were used to infer
816 phylogenetic relationships between periplasmic and epibiotic existing and novel
817 *Pseudobdellovibrionaceae* strains.

818

819 **Table S4. Orthofinder output of gene counts by *Pseudobdellovibrionaceae* isolate in each**

820 **orthogroup.** Rows are predicted orthogroups and columns are genome assemblies. Counts

821 represent the number of gene calls from a genome that belong to a specific orthogroup.

822

823 **Table S5. EggNOG-mapper annotations of each Prodigal-predicted gene in Orthofinder-**

824 **predicted orthogroups.** Each row represents a unique gene identified by Query. Each gene is

825 annotated from a specific *Pseudobdellovibrionaceae* genome and belongs to an orthogroup.

826 Orthogroups may have multiple genes from the same and/or different genomes. Each query has a

827 Seed ortholog that is the best matching sequence in the eggNOG protein space. Genome id is the

828 Prodigal-assigned id to the genome assembly. Input into eggNOG-mapper was the Prodigal faa

829 file output of each genome assembly. Genome names reflect current database names.

830

831 **Supplementary Figures**

832 **Figure S1: Cell shape and predation mode of periplasmic *Pseudobdellovibrionaceae* strains**

833 **MYbb1, MYbb5, MYbb7, MYbb10 and MYbb11.** Stages in the life cycle of periplasmic

834 *Pseudobdellovibrionaceae* isolates are shown on top. Numbers in image corners correspond to

835 the proposed life cycle stage. Stage 1 images represent *Pseudobdellovibrionaceae* cells in attack

836 phase. In stage 2, predators are attached to prey cells (p). After penetration of the prey's outer

837 membrane, *Pseudobdellovibrionaceae* cells enter stages 4-7 with intraperiplasmic growth in

838 bdelloplasts (bd), with one or more predator cells confined within a prey cell (p). Samples were

839 imaged by TEM after negative staining. Scale bar is 500 nm. Life cycle images created in

840 BioRender. Wülbern, J. (2024) BioRender.com/t31h353.

841

842 **Figure S2. Average Nucleotide Identity (a) and Average Amino Acid Identity (b) between**
843 **strains.** Pairwise ANI was calculated with fastANI v1.34 and pairwise AAI was calculated with
844 CompareM v0.1.2. Both were visualized in R with ComplexHeatmap v2.20.0. Novel isolates are
845 listed in bold.

846

847 **Figure S3. Relative frequency of COG categories in orthogroups unique to the core,**
848 **epibiotic, and periplasmic genomes.** Orthogroups were annotated with a COG category using
849 eggNOG-mapper and classified as core (found in all genomes), epibiotic, or periplasmic. Total
850 orthogroups per classification are listed in the figure legend. Relative frequency is calculated by
851 summing COG annotations per category within a classification and divided by the total number
852 of orthogroups per classification.

853

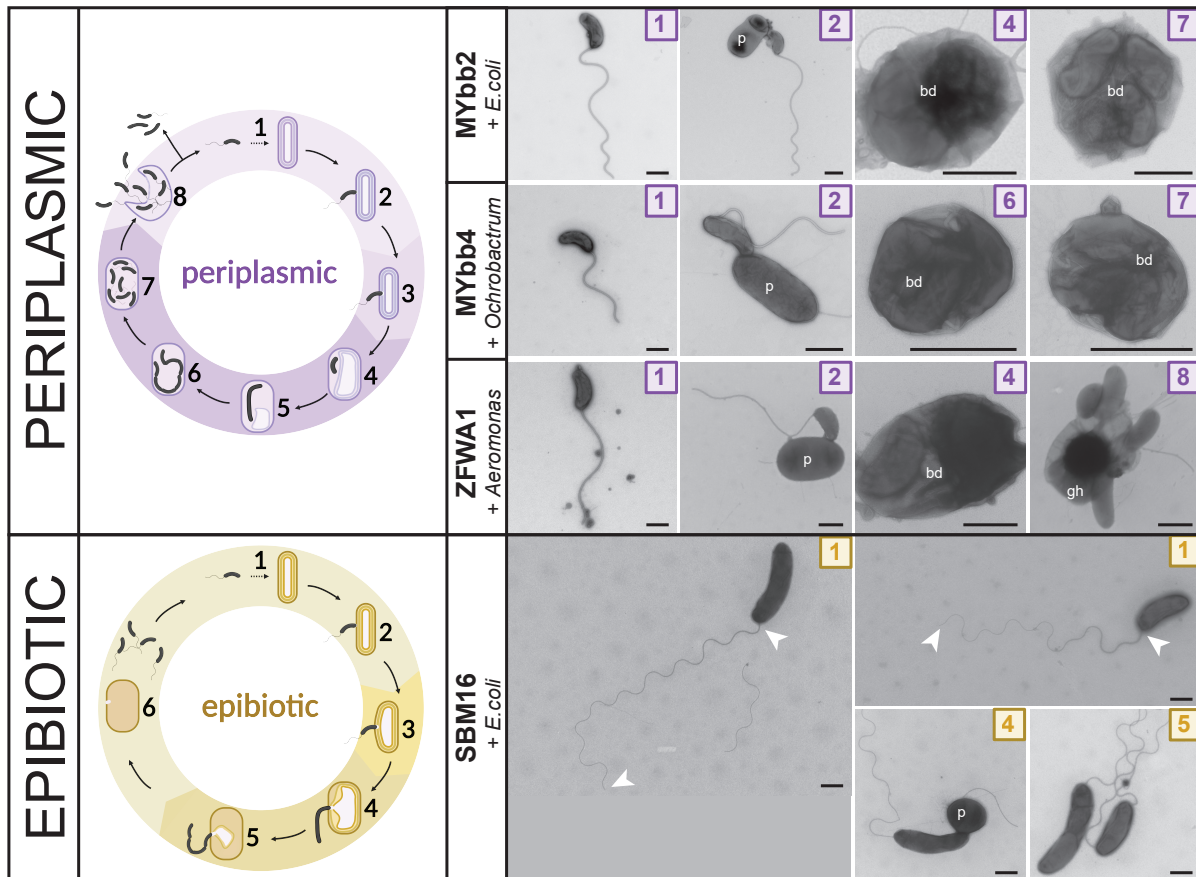


Figure 1: Cell shape and predation mode of *Pseudobdellovibrionaceae* strains MYbb2, MYbb4, ZFWA1 and SBM16. Life cycles of periplasmic (purple) and epibiotic (yellow) *Pseudobdellovibrionaceae* isolates are schematically represented on the left. Numbers in image corners correspond to the proposed life cycle stage. The upper panels illustrate periplasmic *Pseudobdellovibrionaceae* isolates. Stage 1 images represent *Pseudobdellovibrionaceae* cells in attack phase. In stage 2, predators are attached to prey cells (p). Stages 4-7 demonstrate intra-periplasmic growth in bdelloplasts (bd), with one or more *Pseudobdellovibrionaceae* cells confined within the outer membrane of a prey cell. Stage 8 depicts *Pseudobdellovibrionaceae* cells leaving the prey ghost cell (gh). The lower panels display the epibiotic *Bdellovampiro gaculeatus* strain SBM16. This strain has a long flagellum, as illustrated in stage 1 images with white arrows at the start and end point of the flagellum. After attachment to and penetration of the outer membrane, epibiotic cells grow and divide outside prey cells (stages 4-5) as indicated by different sizes of cells and by septation in elongated bacteria. Samples were imaged by TEM after negative staining. Scale bar is 500 nm. Life cycle images created in BioRender. Wülbern, J. (2024) BioRender.com/t31h353.

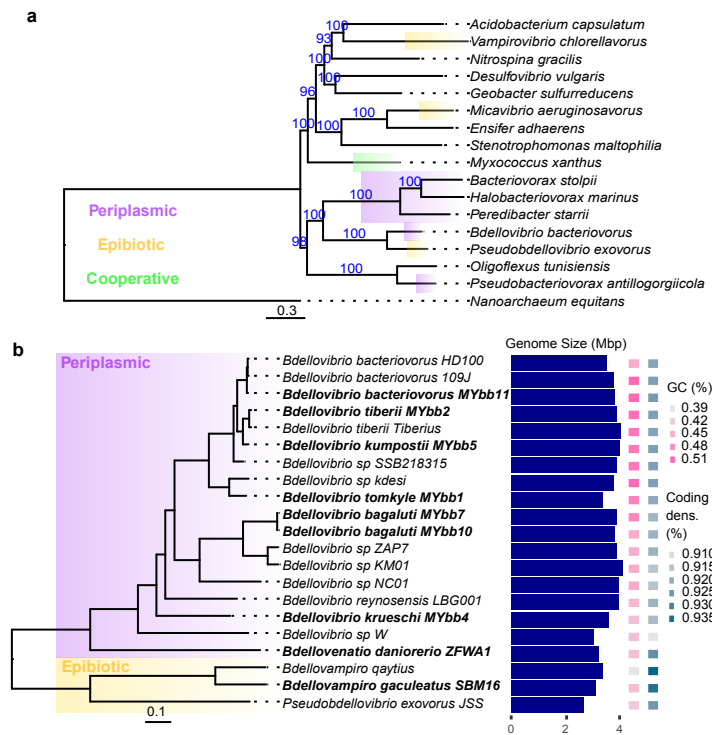


Figure 2. Phylogenetic relationship between various predatory and non-predatory prokaryotes. IQ-TREE was used to infer phylogenetic trees by maximum likelihood with bootstrap approximation. a) Phylogenetic relationships between selected prokaryotic species based on phylogenomic analysis using 265 single-copy genes found in 82.4% of species predicted by Orthofinder. All branch support values are reported in blue. b) Relationships among *Pseudobdellovibrionaceae* strains based on phylogenomic analysis using 1099 single-copy core genes predicted by Orthofinder. All branch support values from bootstrapping approximation were 100. Novel isolates are bolded and listed by the newly proposed names based on 65% AAI genus and 95% ANI species designations.

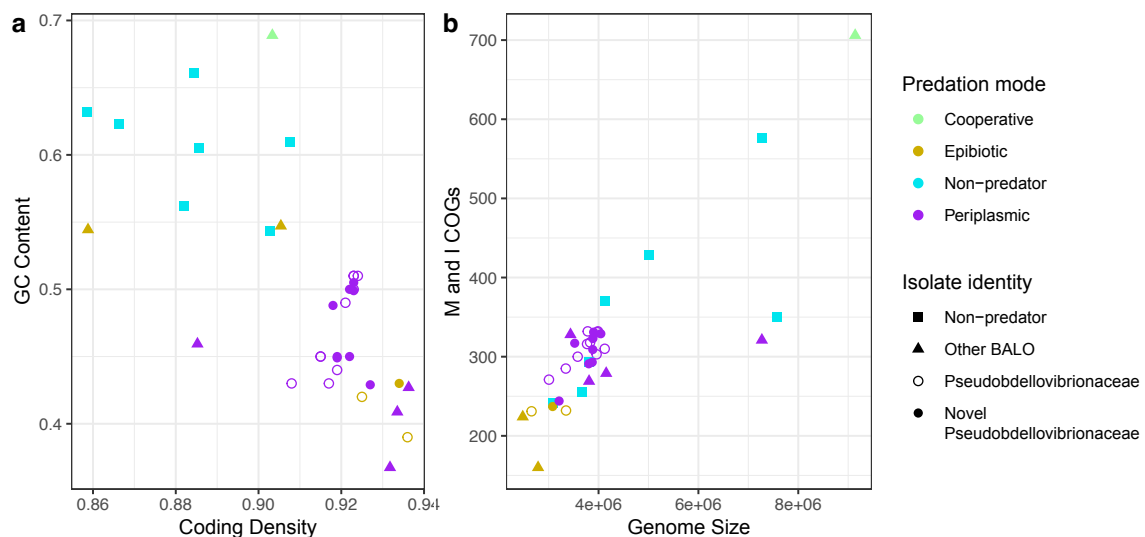


Figure 3. Relationship between different genome metrics of predatory and non-predatory bacteria. a) Relationship between coding density and GC content. b) Relationship between the total combined number of genes in the M (cell envelope biogenesis, outer membrane) and I (lipid metabolism) clusters of orthologous groups (COG) categories and genome size. All bacterial species in Figure 2b are included.

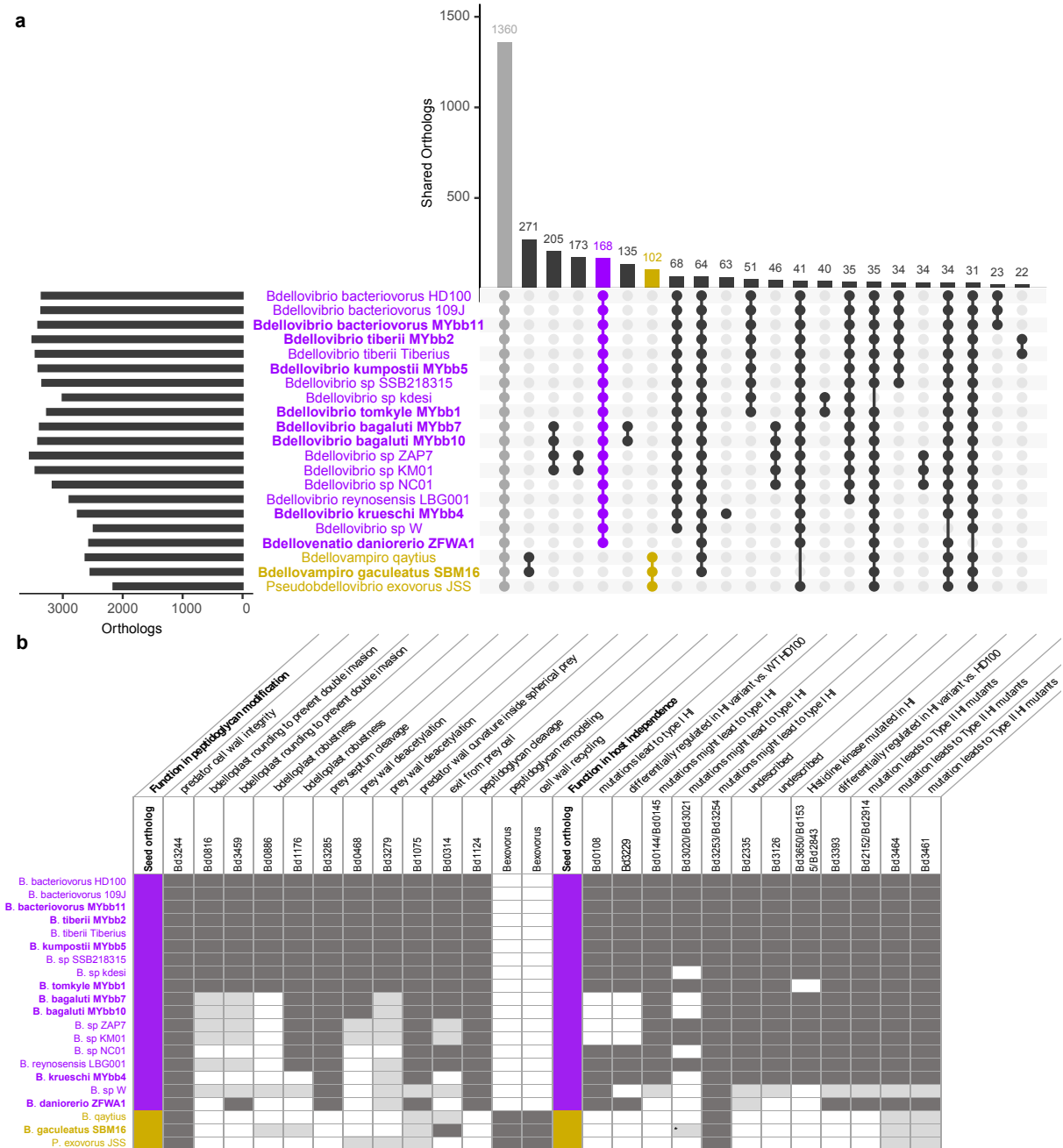


Figure 4. Variation in gene content by predation strategy. a) The number of shared orthologous genes in *Pseudobdellovibrionaceae* strains identified using Orthofinder. The top 22 shared orthologous gene sets are shown. b) Presence of genes involved in peptidoglycan modification and host independence in *Pseudobdellovibrionaceae* isolates. Dark gray cells indicate the presence of the gene with the best protein match listed under seed ortholog. Light gray cells indicate genes with a different seed ortholog that belong in the same orthogroup. The asterisk indicates that only gene Bd3021 is present in SBM16, not Bd3020. All novel isolate names are bolded.

Table 1. Phenotypic characterization of novel *Pseudobdellovibrionaceae* isolates. Values are expressed as mean \pm standard error (MYbb1, MYbb2, MYbb4, ZFWA1) or as mean \pm standard deviation (MYbb5, MYbb7, MYbb10, MYbb11, SBM16). Respective highest/lowest values are highlighted in bold. Measurements for all independent experiments and grids are given in Table S1.

Strain	Species ^a	Flagellum length [μm]	Cell body area [μm^2]	Perimeter [μm]	Feret diameter ratio ^b	Cultivation prey	Predation strategy ^c	Morphology ^d
MYbb11	<i>Bdellovibrio bacteriovorus</i>	2.87 \pm 0.57	0.22 \pm 0.03	1.85 \pm 0.17	1.81	<i>E.coli</i>	periplasmic	
MYbb2	<i>Bdellovibrio tiberii</i>	3.34 \pm 0.36	0.25 \pm 0.04	2.01 \pm 0.2	1.92	<i>E.coli</i>	periplasmic	
MYbb5	<i>Bdellovibrio kumpostii</i>	3.02 \pm 0.55	0.21 \pm 0.03	1.9 \pm 0.16	2.08	<i>E.coli</i>	periplasmic	narrow cell
MYbb1	<i>Bdellovibrio tomkyle</i>	3.02 \pm 0.22	0.19 \pm 0.02	1.67 \pm 0.1	1.78	<i>E.coli</i>	periplasmic	
MYbb7	<i>Bdellovibrio bagaluti</i>	2.99 \pm 0.44	0.21 \pm 0.03	1.82 \pm 0.19	2.01	<i>E.coli</i>	periplasmic	
MYbb10	<i>Bdellovibrio bagaluti</i>	2.9 \pm 0.34	0.29 \pm 0.04	2.36 \pm 0.21	2.29	<i>E.coli</i>	periplasmic (no confirmation)	narrow cell
MYbb4	<i>Bdellovibrio krueschi</i>	2.58 \pm 0.33	0.25 \pm 0.03	2.15 \pm 0.2	2.16	<i>Ochrobactrum sp.</i>	periplasmic	short flagellum, narrow cell
ZFWA1	<i>Bdellovibrio daniorerio</i>	2.77 \pm 0.25	0.25 \pm 0.05	1.99 \pm 0.2	1.9	<i>Aeromonas sp.</i>	periplasmic	
SBM16	<i>Bdellovibrio gaculeatus</i>	7.13 \pm 1.57	0.77 \pm 0.24	4.33 \pm 0.97	3.24	<i>E.coli</i>	epibiotic	long flagellum, narrow cell

^aSpecies named according to results of comparative genome analysis, see section below for details.

^bThe Feret diameter ratio was used as a proxy for cell size and shape, with higher values indicating elongated cells.

^cPhenotype confirmed by TEM imaging after negative staining.

^dDescription for strains with outstanding phenotype.

Table 2. Genome comparison of novel *Pseudobdellovibrionaceae* isolates with *Bdellovibrio* and *Pseudobdellovibrio* type strains. Genome quality estimates of % completion (% comp.) and % contamination (% cont.) were obtained from Checkm2. The number of coding genes (CDS) and different types of RNA genes were predicted using Prokka. Exclusively present orthogroups (OG) defined by Orthofinder were only found in a single genome, and exclusively absent orthogroups were found in all genomes but one. Novel isolates are bolded, and type strains are indicated with an asterisk.

	Genome size	GC content (%)	# of contigs	% comp.	% cont.	CDS	tRNA	rRNA	Other RNA	Exclusively present OG	Exclusively absent OG
<i>Bdellovibrio bacteriovorus</i> HD100*	3,782,950	50.6	1	99.99	0.15	3,563	36	6	1	0	1
<i>Bdellovibrio bacteriovorus</i> strain MYbb11	3,901,330	50.5	1	100	0.34	3,647	36	6	1	0	0
<i>Bdellovibrio tiberii</i> strain MYbb2*	4,045,310	49.8	19	100	0.34	3,821	35	3	1	3	1
<i>Bdellovibrio kumpostii</i> strain MYbb5*	3,886,825	49.9	1	100	0.28	3,672	35	6	1	1	0
<i>Bdellovibrio tomkyle</i> strain MYbb1*	3,884,186	48.8	1	100	0.25	3,702	37	6	1	2	1
<i>Bdellovibrio bagaluti</i> strain MYbb7*	3,803,878	45	1	99.99	0.88	3,689	34	6	1	1	0
<i>Bdellovibrio bagaluti</i> strain MYbb10	3,873,366	44.9	1	99.99	0.84	3,754	34	6	1	0	0
<i>Bdellovibrio krueschi</i> strain MYbb4*	3,522,424	45.2	5	99.95	11.38 ^a	3,479	38	6	2	63	7
<i>Bdellovibrio daniorerio</i> strain ZFWA1*	3,209,714	42.9	4	99.98	0.79	3,082	38	6	1	17	31
<i>Bdellovampiro gaculeatus</i> strain SBM16*	3,080,354	43.5	16	97.12	0.76	2,885	31	4	1	3	2
<i>Pseudobdellovibrio exovorus</i> JSS*	2,657,893	41.9	1	99.99	0.4	2,616	33	3	0	14	64

^aOther programs reported deviating levels of contamination, including checkm1 (5.41%), BUSCO (3.2%), and NCBI fcs-gx (0%)

Table 3: *Pseudobdellovibrionaceae* strains can be found in 16S rDNA data sets of relevant hosts. Number of the different *Pseudobdellovibrionaceae* ASVs with up to 4 mismatches (i.e. 99% identity) and their prevalence are shown for each microbiome study and all *Pseudobdellovibrionaceae* strains used in this study.

Host microbiome	ZFW strain	SBM strain	MYbb strains	Other, aquatic strains	Other, terrestrial strains	Total prevalence in organisms
Zebrafish ^a				JSS in 1/29 samples ⁰		1 ASVs in 1/29 samples (3.5%)
Zebrafish ^b	1 ASV in 78/210 samples ⁰			2 ASVs: ZAP ² , JSS ³ each in 1/210 samples		4 ASVs in 79/210 samples (37.6%)
Zebrafish ^c	2 ASVs in 4/384 samples ^{0,1}					2 ASVs in 3/384 samples (0.8%)
Stickleback ^d		2 ASVs: in 2/296 samples ⁰ & in 7/296 samples ²				2 ASVs in 9/296 samples (3%)
Stickleback ^e	1 ASV in 104/145 samples ⁴	1 ASV in 11/145 samples ⁰	2 ASVs: MYbb4 in 42/145 samples ² , MYbb1 in 2/145 samples ¹	JSS in 9/145 samples ⁴		5 ASVs in 116/145 samples (80%)
Worm ^{f,*}			✓	✓	✓	4 ASVs in 7/361 samples (2%)
Worm ^{g,*}			✓	✓	✓	7 ASVs in 8/257 samples (3.1%)

⁰⁻⁴: number of mismatches to reference sequences

^aSkin and gut samples collected in 2018 from wildtype adult zebrafish (238 days post fertilization or dpf) reared at the University of Oregon Zebrafish Facility under standard husbandry conditions. Unpublished. Sequenced 16S rRNA region: V4.

^bEgg samples from 0, 1, and 2 dpf wildtype zebrafish collected in 2022 at the University of Oregon Zebrafish Facility under standard husbandry conditions. Unpublished. Sequenced 16S rRNA region: V4.

^cEgg (0 and 2 dpf) and larval gut (5 and 7 dpf) samples from wildtype zebrafish collected in 2023 at the University of Oregon Zebrafish Facility under standard husbandry conditions. Unpublished. Sequenced 16S rRNA region: V4.

^dGut samples collected in 2016 from juvenile threespine stickleback (60dpf) reared at the Cresko Stickleback facility at the University of Oregon under standard husbandry conditions. Published in [60]. Sequenced 16S rRNA region: V4.

^eGut samples collected in 2015 from adult male threespine stickleback (12-16 months) reared at the Cresko Stickleback facility at the University of Oregon under standard husbandry conditions. Published in [61]. Sequenced 16S rRNA region: V4.

^fNatural worm samples collected from a compost heap in 2016-2017 and published in [62]. Sequenced 16S rRNA region: V3-V4.

^gNatural worm samples collected from apples on a compost heap in 2019-2020 and published in [63]. Sequenced 16S rRNA region: V3-V4.

*multiple ASVs in worm samples matched similarly well to multiple *Pseudobdellovibrionaceae* strains